Ceramics International 31 (2005) 591–598

CERAMICS INTERNATIONAL

www.elsevier.com/locate/ceramint

Preparation and characterization of silica-doped aluminum nitride–aluminum nitride polytypoid composites

Inger-Lise Tangen[a], Yingda Yu[b], Tor Grande[a], Ragnvald Høier[b], Mari-Ann Einarsrud[a,*]

[a]*Department of Materials Technology, Norwegian University of Science and Technology, 7491 Trondheim, Norway*
[b]*Department of Physics, Norwegian University of Science and Technology, 7491 Trondheim, Norway*

Received 5 April 2004; received in revised form 17 May 2004; accepted 24 June 2004
Available online 25 September 2004

Abstract

Fine-grained AlN–AlN polytypoid composites doped with SiO_2 were prepared in situ by pressureless sintering of AlN–Al_2O_3 mixtures (3.7 and 10.5 mol% Al_2O_3) at 1870 °C using Y_2O_3 as sintering aid. SiO_2-doping (1 wt.%) was used to stabilize the AlN polytypoids and reduce the average grain size of the polytypoids. The composites consisted of elongated SiO_2 containing AlN polytypoids grains (30 and 61 vol.%) embedded in equi-axed AlN matrix. Vickers hardness and bending strength increased with polytypoid composite formation. The Young's modulus showed a maximum at 3.7 mol% Al_2O_3 (30 vol.% polytypoids). The fracture toughness increased up to 4.0 ± 0.3 MPa $m^{1/2}$ for the composites. The toughening was caused by crack deflection due to residual strain both in the polytypoids and the AlN matrix.

Keywords: A. Grain growth; B. Microstructure-final; C. Mechanical properties; D. SiAlON

1. Introduction

Aluminum nitride (AlN) polytypoids are formed at high temperatures (>1881 ± 6 °C) in the aluminum nitride-aluminum oxide (AlN–Al_2O_3) system [1–5]. The polytypoids are also known as AlN compositional polytypes due to their oxygen content. The structure has recently been described as arrays of alternating planar (oxygen containing) and corrugated (without oxygen) inversion domain boundaries (IDBs) in AlN [6,7]. As AlN polytypoids grow as elongated or plate-like grains, [8,9] in situ formation of composite materials consisting of polytypoid grains in an AlN matrix might represent an effective route to toughen AlN ceramics. Increased fracture toughness is probably necessary to initiate the use of AlN ceramics in high temperature structural applications. Si_3N_4 and SiC are examples of ceramics showing highly increased fracture toughness by in situ grown elongated grains. The formation of hexagonal β-Si_3N_4 and α-SiC during sintering have increased the fracture toughness of Si_3N_4 and SiC up to 10 and 8–9 MPa $m^{1/2}$ [10,11], significantly higher than the fracture toughness reported for AlN, 3–4 MPa $m^{1/2}$ [12–17].

Huang and Jih [13,18] reported an increasing fracture toughness and Vickers hardness and decreasing fracture strength as platelike AlN polytypoids were formed during hot-pressing of pure AlN and AlN–SiC materials at and above 2100 °C. Also Kuzenkova et al. [19] and Tkachenko et al. [20] have reported reinforcement of AlN composites (con- taining TiN, TiO_2, $MoSi_2$, TiC, etc.) by formation of polytypoid-like grains. Sakai [21] studied the relation between phase composition and bending strength for hot-pressed AlN–Al_2O_3 materials and found that polytypoids in moderate volume fractions increased the bending strength, but in larger fractions the bending strength was decreased. AlN–AlN polytypoid composites in the Y_2O_3–AlN–Al_2O_3 system have been prepared and characterized by Tangen et al. [5].

---

* Corresponding author. Tel.: +47 73 59 4002; fax: +47 73 59 0860.
E-mail address: mari-ann.einarsrud@material.ntnu.no
(M.-A. Einarsrud).

0272-8842/$30.00 © 2004 Elsevier Ltd and Techna Group S.r.l. All rights reserved.
doi:10.1016/j.ceramint.2004.06.026

It is well known that addition of silicon oxide (SiO_2) lowers the stability temperature for AlN polytypoids and existence down to 1400 °C is reported in the SiAlON system [6,8,22–25]. Westwood et al. [6] compared the detailed structure of the polytypoids formed in pressureless sintered AlN–Al_2O_3 mixtures with and without SiO_2-addition ($\leq$1 wt.%). In the SiO_2 doped samples the amount of polytypoids was higher compared to the SiO_2-free samples and the number of isolated IDBs in the AlN grains decreased abruptly. The mechanical properties of AlN polytypoids containing SiO_2 have been studied, but only a small dependence on the oxygen content of the polytypoids was reported [8,26,27].

In this work we have taken advantage of the increased stability of AlN polytypoids by minor SiO_2 doping and developed fine-grained AlN–AlN polytypoid composites with elongated polytypoid grains in an AlN matrix. The composites were prepared by pressureless sintering using Al_2O_3–Y_2O_3 as sintering additive. A systematic study of the influence of SiO_2 on microstructure, sintering mechanism and kinetics of the polytypoid formation is discussed. Finally, the mechanical properties are investigated and the possibility for toughening of AlN ceramics due to elongated polytypoid grains is addressed.

2. Experimental

The composite materials were prepared from AlN powder (Tokuyama Soda, Grade F, containing 0.6 wt.% oxygen on the grain surface), Al_2O_3 (Alcoa, A 16 SG) (3.7 and 10.5 mol% (assuming only AlN and Al_2O_3)) and fine SiO_2 (1 wt.%) prepared as described by Hæreid et al. [28] Y_2O_3 (H.C. Starck, quality Finest) (1.4 wt.%) was added to form sintering aid with Al_2O_3. Pure AlN materials containing 0.2 mol% Al_2O_3 and 0.9 wt.% Y_2O_3 as sintering additives were prepared from the same starting powders.

The powders were mixed in 100% ethanol by ball milling for four hours using alumina balls. Soft agglomerates (<500 μm) were formed by sieving before preparation of green bodies. The powder was pressed into bars, first uniaxially pressed at 15 MPa and then isostatically pressed at 200 MPa. Ethyl cellulose (Sigma) (2 wt.%) was used as binder. The green density of the bars was approximately 56%.

The ceramics were sintered in static N_2-atmosphere in a graphite resistance furnace described by Herstad and Motzfeldt [29]. The sample temperature was measured using an automatic pyrometer (Model PZ20-AF5, Keller GmbH). The composites were sintered in AlN powder bed in silicon carbide (SiC) crucibles with lids for two hours at 1870 °C. The heating and cooling rate was 300 K/h. The pure AlN samples were sintered in molybdenum (Mo) lined graphite crucibles at 1870 °C for six hours. The density was determined by Archimedes' method using isopropanol. The amount of polytypoids was measured by determination of the area fraction of polytypoids in SEM images. Based on the estimated content of polytypoids, the composition of the remaining part of the materials was calculated, assuming pure AlN, Al_2O_3 and Y_2O_3 to be the other phases. The theoretical density was calculated from the law of mixtures based on the calculated phase composition and was not corrected for weight loss during firing.

The microstructure of the samples was studied by optical microscopy (Reickert MeF3 A), scanning electron microscopy (SEM) (Hitachi S3500N) with fitted energy dispersive spectroscope (EDS) (Oxford Instruments Model 7021) and transmission electron microscopy (TEM)/high resolution TEM (HRTEM) (Philips CM30). Phase composition was studied by powder X-ray diffraction (XRD) using a Siemens D5005 X-ray diffractometer. The samples were ground to powder using a boron carbide mortar prior to XRD measurements. The AlN grain size was measured by the linear intercept method on polished and thermally etched (1600 °C for 0.2 h) surfaces. A total of approximately 400 grains were measured for each sample. The aspect ratio of the polytypoid grains was calculated by measuring the maximum and minimum diameter of the grains from SEM images of polished samples. The average aspect ratio was estimated as the mean value of the 10% highest observed aspect ratios [30]. In total 200–250 elongated grains were measured for each sample.

Bending strength and Young's modulus (E-modulus) were measured using a four point bending test (40/20 mm span). Sample bars were machined to MIL SPEC 1942 and dimensions 4 mm × 3 mm × 45 mm by Chand Associates, MA, USA. All the edges were chamfered. The calculation of Young's modulus was based on an equation describing the deflection of the bar, reported by Sass et al. [31]. A total of 6–11 specimens were tested for each composition. The fracture surfaces were studied by SEM to reveal the fracture origins. The fracture toughness was determined using the single edge notched beam method (SENB). The sample bar dimensions used were 4 mm × 3 mm × 45 mm, the depth of the notches was 1.2 mm and the width about 0.2 mm. Fracture toughness was calculated using ISO 15732 [32]. A total of 4 specimens were tested for each composition. The fracture toughness was also determined at room temperature and at 800 °C in flowing N_2-atmosphere (max 200 ppm O_2). Both 4-point bending and the SENB testing were performed by 4-point flexure 40/20 mm span in a high temperature mechanical testing rig described previously [33]. The room temperature mechanical testing of pure AlN is also described previously [34]. All measurements were performed in displacement control at a crosshead rate of 8 μm/s. Hardness was measured using the Vickers indentation method on polished surfaces. An Akashi AVK-C1 Hardness Tester was used for the indentation and a Reickert MeF3 A optical microscope with a Sony DXC-930P Colour Video Camera and the program NIH Image for measuring the indentations. The hardness

Table 1
Phases identified by XRD and HRTEM in SiO_2-doped AlN–AlN polytypoid composites

Al_2O_3 (mol%)	XRD				HRTEM
	AlN	Spinel (γ-AlON)	YAG	AlN polytypoids	
3.7	+ + + +	(+)	+	+ + (27R)	27R IG[a]: 20H, 27R, 21R
10.5	+ + +	+	+	+ + + (27R, 21R)	27R, 16H and 21R IG[a]: 27R, 16H, 21R

+ + + + main phase; + + + large amounts;+ + medium amounts; + small amounts; (+) traces.

[a] IG: intergrowth.

was calculated using the equation reported by Anstis et al. [35].

3. Results

The AlN–AlN polytypoid composites obtained high density (>99.0%) and low weight loss after sintering, approximately 0.5% for both composites. The phases identified by XRD and HRTEM and their semi-quantitative amounts are given in Table 1. Both composites contain AlN and polytypoids as the major phases and the polytypoid content increases considerably when increasing the Al_2O_3 content. In addition yttria alumina garnet (YAG, $Al_5Y_3O_{12}$) is identified in both materials. YAG solidifies from the AlN containing Y_2O_3–Al_2O_3 liquid during cooling. According to the binary Al_2O_3–Y_2O_3 system and the quaternary Al_2O_3–Y_2O_3–AlN–YN system, YAG is stable at low temperatures with a low solubility of nitrogen [36,37]. Formation of YAG is reported to be favored by SiO_2 [25]. Only traces of spinel (γ-AlON) are identified in the 3.7 mol% Al_2O_3 material while a small amount is identified in the 10.5 mol% Al_2O_3 material. The main AlN polytypoids are identified by XRD as 27R in the 3.7 mol% Al_2O_3 material and 27R and 21R in the 10.5 mol% Al_2O_3 material. HRTEM was further used to identify the polytypoids and 16H was found in addition to 27R and 21R in the 10.5 mol% Al_2O_3 material. Intergrowth of several different polytypoids was also observed. The average oxygen content of the polytypoid phases increased with increasing Al_2O_3 content in the materials and the average Ramsdell number decreased in line with the nominal composition. The polytypoid containing least oxygen was 20H, identified in intergrowth in the 3.7 mol% Al_2O_3 ceramic.

SEM images showing fracture surfaces and polished surfaces of the two composite materials are given in Fig. 1. The fracture surfaces (Fig. 1a and c) show mainly transgranular fracture. A small number of elongated poly-

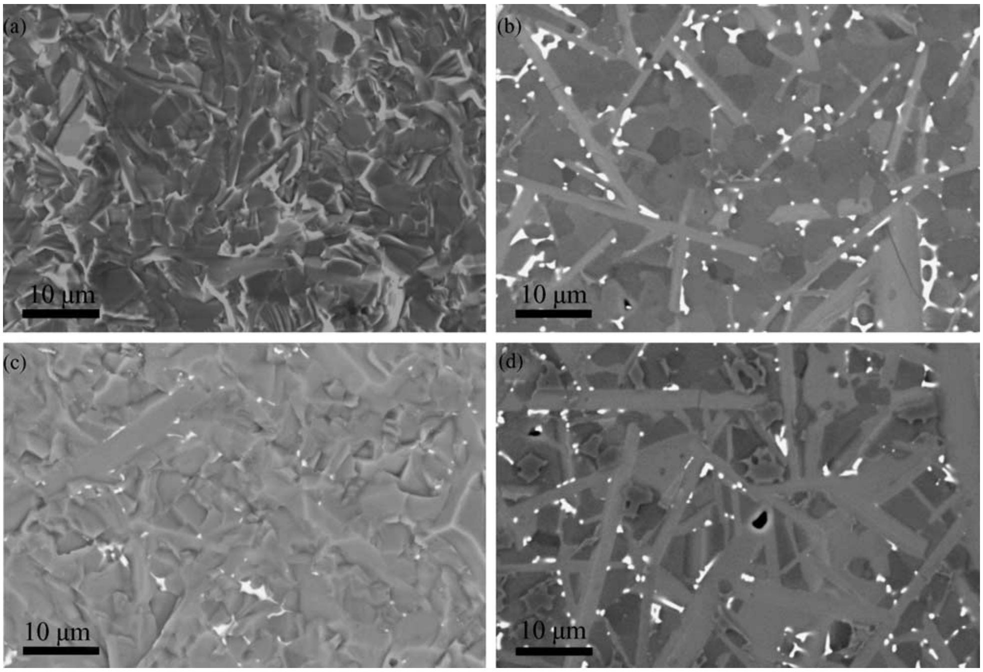

Fig. 1. Fracture surfaces from SENB-testing (room temperature, air) and backscatter SEM images of polished surfaces of SiO_2-doped AlN–AlN polytypoid composites: (a and b) 3.7 mol% Al_2O_3 material, (c and d) 10.5 mol% Al_2O_3 material.

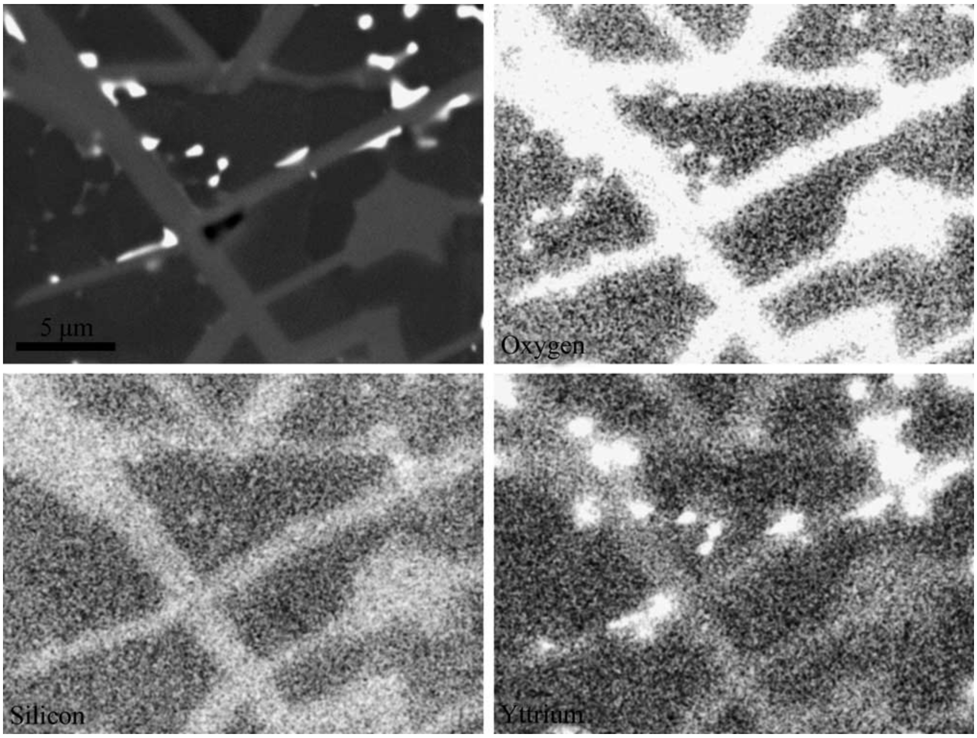

Fig. 2. Elemental mapping showing the content of oxygen, silicon and yttrium in a SiO_2-doped AlN–AlN polytypoid composite containing 3.7 mol% Al_2O_3.

typoid grains are observed, also these exhibit a transgranular fracture mode. The elongated grains are more easily seen in the backscatter images from polished surfaces (light contrast in Fig. 1b and d) and the number of elongated grains is lower for the 3.7 mol% Al_2O_3 material compared to the 10.5 mol% material. Dark contrast equi-axed AlN grains surround the polytypoid grains and spinel (γ-AlON) is observed as irregularly shaped medium gray contrast grains in-between the polytypoid and AlN grains in the 10.5 mol% Al_2O_3 material (Fig. 1d). The light contrast YAG phase is situated at grain boundaries and triple junctions. The grain size of AlN in the composite materials is about 3 µm and the grain growth is clearly restricted by the polytypoid grains, especially in the 10.5 mol% Al_2O_3 material. The aspect ratio of the AlN polytypoid grains is 18 ± 7 and 15 ± 4 for the 3.7 and 10.5 mol% Al_2O_3 materials, respectively. The main growth direction of the polytypoid grains is along the hexagonal *a*-axis, found by combining low magnification TEM and HRTEM.

Neither XRD nor microstructural studies identify any SiO_2-based phases in the composite materials. Using elemental mapping, shown in Fig. 2, silicon is detected in the polytypoids. Besides the silicon a small amount of yttrium is identified in the polytypoids, as observed previously in AlN–AlN polytypoid composites in the Y_2O_3–Al_2O_3–AlN system without SiO_2 addition [5].

As the Al_2O_3 content of the composites is increased, the amount of polytypoid phases increases. In Fig. 3 the measured polytypoid amount is plotted versus Al_2O_3 content and compared to the theoretical polytypoid amount based on the phase relation in a binary section in the AlN–Al_2O_3–Y_2O_3 system [5]. The theoretical polytypoid amount assuming 27R to be the stable polytypoid with lowest oxygen content is also included. The measured polytypoid content is considerably lower than theoretical and shows that equilibrium is not reached. However, if 27R is assumed to be the AlN polytypoid with lowest oxygen content, near equilibrium amount of polytypoids is formed in the 3.7 mol% Al_2O_3 composite.

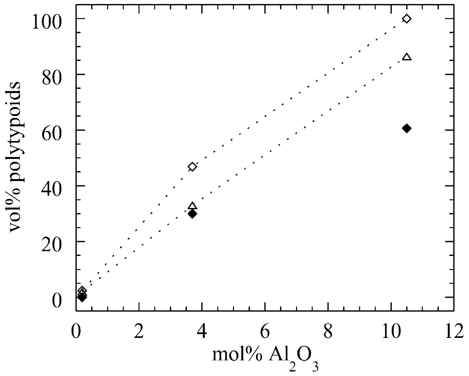

Fig. 3. Calculated vol.% polytypoids in SiO_2-doped AlN–AlN polytypoid composites (filled diamonds) plotted versus total mol% Al_2O_3. The open diamonds and triangles are vol.% polytypoids calculated based on AlN–Al_2O_3 composition join proposed by Tangen et al. [5], assuming 39R or 27R, respectively, to be the stable polytypoid with lowest oxygen content at 1870 °C in the SiO_2-doped AlN–Al_2O_3 system.

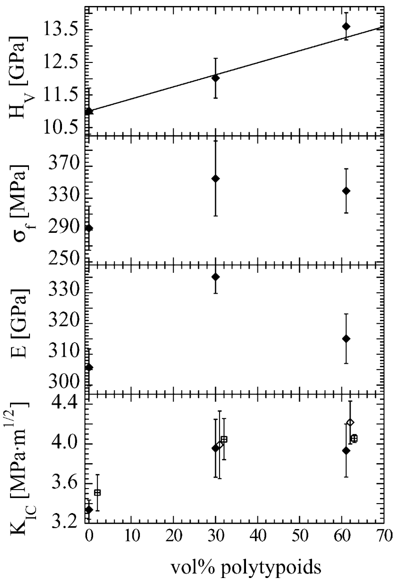

Fig. 4. Vickers hardness, 4-point bending strength, E-modulus and fracture toughness (SENB method) of AlN and SiO_2-doped AlN–AlN polytypoid composites versus polytypoid contents. 30 vol.% polytypoid corresponds to the 3.7 mol% Al_2O_3 material, 61 vol.% polytypoid corresponds to the 10.5 mol% Al_2O_3 material. The line in the hardness plot is the linear mixing between Vickers hardness for pure AlN and pure SiO_2 containing 27R [26]. The filled diamonds are measurements performed at room temperature and in air. The open diamonds are measurements performed at room temperature in N_2 atmosphere and the open squares are measurements performed at 800 °C in N_2 atmosphere. The different symbols in the fracture toughness plot are shifted for easier reading. The error bars represent the standard deviation.

The pure AlN material has described in a previous work [30]. The material consisted of equi-axed AlN with grain size 7 ± 1 μm, and YAG was situated at grain boundaries and triple junctions. The relative density was 99.1 ± 0.2%.

4. Mechanical properties

Vickers hardness, 4-point bending strength, Young's modulus (E-modulus) and fracture toughness of the AlN–AlN polytypoid composites at room temperature are presented in Fig. 4. Fracture toughness in N_2-atmosphere at room temperature and 800 °C is also included. The Vickers hardness of the composite materials increases strongly with Al_2O_3 and polytypoid content. The hardness is close to the theoretical hardness for AlN–AlN polytypoid composites calculated by linear mixing based on hardness for the pure materials. The hardness reported for SiO_2 containing 27R by van Tendeloo et al. [26], 14.7 GPa, was used as a theoretical hardness for the polytypoids. Increasing hardness with increasing polytypoid content also corresponds to results from hot-pressed AlN-materials [13]. The hardness of the composites is slightly higher than reported for AlN–AlN polytypoids without SiO_2-doping [5].

The bending strength of pure AlN, 281 ± 39 MPa, is in good agreement with literature values, [13,14,16,38] and is significantly increased when AlN–AlN polytypoid composites are formed. The bending strength of the composites, 354 ± 47 MPa and 339 ± 27 MPa, are high compared to the bending strength of 313–366 MPa (3-point testing) reported for pure Si-containing polytypoids (15R, 12H and 21R) [27]. The increasing bending strength with polytypoid formation is contradictory to what is reported by Huang and Jih [13] and Sakai [21] for SiO_2-free AlN polytypoid-containing materials. The fracture origins were identified as either pores or large grains. The pores are formed either from volatile contaminations or inhomogeneous packing of the green body.

The Young's modulus increases when polytypoids are formed and a maximum is reached (335 ± 5 GPa) for the 3.5 mol% Al_2O_3 material. The E-modulus for the 10.5 mol% Al_2O_3 material is only slightly higher than the pure AlN

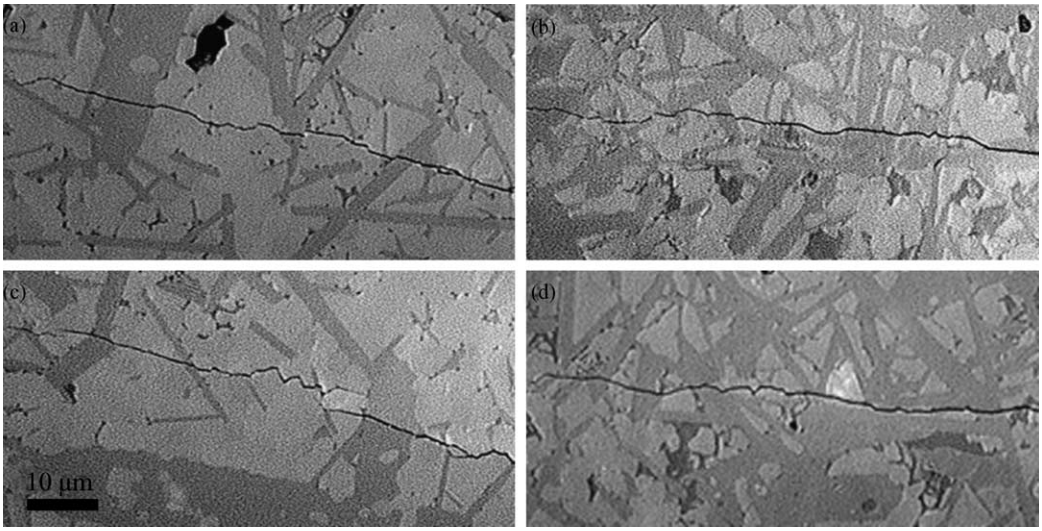

Fig. 5. Optical images showing cracks from high load Vickers indentations (49.05 N) in SiO_2-doped AlN–AlN polytypoid composites. The cracks propagate towards the left of the images: (a and c) 3.7 mol% Al_2O_3 material, (b and d) 10.5 mol% Al_2O_3 material.

material (306 ± 6 GPa and 315 ± 8 GPa, respectively). Both values are in the range of what is reported for AlN [12,14,38,39].

The fracture toughness of AlN exhibits a significant increase when polytypoid composites are formed. At room temperature (in air) the fracture toughness increases to 4.0 ± 0.3 MPa $m^{1/2}$ for the composites. No difference in fracture toughness was observed between the 3.7 mol% Al_2O_3 and the 10.5 mol% Al_2O_3 materials. All the measurements performed in N_2 atmosphere resulted in slightly higher fracture toughness than the ones performed in air, but no trend was observed when increasing the temperature and retaining the N_2 atmosphere. The measured fracture toughness of the composites was somewhat lower than what was reported by Wang et al. [27] for pure high-oxygen SiO_2 containing polytypoids (15R, 12H and 21R), but considerably higher than what van Tendeloo et al. [26] reported for low-oxygen SiO_2 containing polytypoids (>27R). The fracture toughness of the composites was also high compared to reported fracture toughness for AlN [12–17].

The fracture surfaces from mechanical testing exhibited a mainly transgranular fracture mode, except pure AlN fractured in air at room temperature, where a large fraction of intergranular fractures was observed. In Fig. 5 examples of crack propagation from high load Vickers indentation are shown. The cracks propagate transgranular through both AlN and polytypoid grains. Crack deflection is observed, but the fluctuations are smaller than the measured grain size.

5. Discussion

5.1. Stabilization of polytypoid phases

Due to the lower stability temperature of the AlN polytypoids in the SiO_2–AlN–Al_2O_3(–Y_2O_3) system, dense SiO_2-doped polytypoid composites can be prepared in situ using a lower firing temperature compared to AlN–Al_2O_3(–Y_2O_3) polytypoid composites. The weight fraction of polytypoids is considerably higher for SiO_2-doped materials compared to AlN–Al_2O_3(–Y_2O_3) materials with similar oxygen content [5,6,8]. Y_2O_3 addition is reported to cause non-equilibrium and low polytypoid content in both AlN–Al_2O_3(–Y_2O_3) and SiO_2–AlN–Al_2O_3(–Y_2O_3) materials [5,23,40–42]. Tangen et al. [5] explained the deviation from equilibrium phase content by the combination of low nucleation rate and rapid grain growth of polytypoids in the liquid Al_2O_3–Y_2O_3 phase. In SiO_2 containing materials the sintering temperature is decreased and the nucleation rate is expected to increase. Increased nucleation rate will give a high number density of polytypoid grains in the SiO_2-doped materials contributing to bring the system closer to equilibrium and simultaneously reduce the average grain size of the polytypoids.

The identified polytypoids in the SiO_2-doped AlN–Al_2O_3 materials (Table 1) have higher oxygen content than the polytypoids in Si-free AlN–Al_2O_3–Y_2O_3 materials with a corresponding total Al_2O_3 content. In the SiO_2-doped materials the polytypoid with lowest oxygen content identified in intergrowth is 20H and as single phase 27R. Polytypoids with lower oxygen content are reported in the SiO_2–AlN–Al_2O_3 system, but either at higher temperatures or in materials containing a larger amount of SiO_2 [13,25,26]. According to Tangen et al. [5] the decomposition temperature of SiO_2-free AlN polytypoids in the AlN–Al_2O_3–Y_2O_3 system increases with decreasing oxygen content. If a similar trend holds for the SiO_2-doped polytypoids, it is likely that the polytypoids containing less oxygen than 20H or 27R are not stable at the firing temperature (1870 °C) and are therefore not formed during sintering. Assuming 27R to be the stable polytypoid with the lower oxygen content instead of 39R, (open triangles in Fig. 3), the achieved polytypoid content for the 3.7 mol% Al_2O_3 material is close to equilibrium. This corresponds well with the XRD-results as the 3.7 mol% Al_2O_3 material contains only traces of spinel (γ-AlON) while the 10.5 mol% Al_2O_3 material has not reached equilibrium, and contains a small amount of spinel (γ-AlON).

5.2. Mechanical properties

The bending strength of the composite materials is higher than for pure AlN materials, probably caused by the increasing fracture toughness. The Vickers hardness is in good agreement with the linear mixing of AlN and SiO_2 containing AlN polytypoid as expected from a homogenous, fine-grained material. The Young's modulus of the 3.7 mol% Al_2O_3 SiO_2-doped composites is higher than the other two materials, pure AlN and 10.5 mol% Al_2O_3. A corresponding maximum is however, not observed in bending strength or fracture toughness. Both the microstructure and the phase composition of the two composite materials are comparable, only the fraction of elongated polytypoid grains is different. The elastic extension of a body is directly related to the interatomic forces and the structure energy and a monotonous increase/decrease in the E-modulus is expected for a two-phase composite material when changing the ratio between the two phases [43].

The fracture toughness is higher in the materials containing polytypoids compared to the pure AlN material. Regardless of the improved toughness, no distinct toughening mechanisms are observed on the microstructural scale and the crack proceeds through the polytypoid grains as well as the AlN grains with only small deflections (Fig. 5). The toughening effect is crack deflection due to preferred crack growth in specific atomic planes and strain in the matrix due to thermal expansion or elastic mismatch. The pure AlN ceramics exhibit an increase in transgranular fractures from room temperature to 800 °C. Despite this change, the fracture toughness shows a minor increase indicating that crack deflection due to preferred crack growth in specific atomic planes is an important toughening mechanism in

Al_2O_3–Y_2O_3 liquid phase sintered AlN ceramics. Corresponding crack deflection is reported for both AlN–TiN and AlN–SiC particulate composites and AlN–AlN polytypoid composites [5,30,34]. As the fracture toughness increases with decreasing average grain size, residual strain has to give significant contribution to the toughening in the polytypoid composites. In addition, the elongated polytypoid grains will increase the toughening effect of residual strain due to the more anisotropic properties compared to equi-axed secondary particles.

No significant differences in fracture toughness between the two different materials prepared are observed. Tangen et al. [5] reported a fracture toughness maximum for SiO_2-free composites at 10.5 mol% Al_2O_3, corresponding to 32 vol.% polytypoids. The mutual conclusion of these two studies is that the fracture toughness can be increased by formation of polytypoids up to approximately 30 vol.% polytypoids, above which no changes are observed. Faber and Evans [44,45] reported an analogous limit, in studies of the toughening effect of crack deflection due to secondary particles. Further toughening of AlN by elongated polytypoids will be dependent on optimization of the grain size and grain boundary phases.

6. Conclusion

SiO_2-doped AlN–AlN polytypoid composite materials have been formed in situ by pressureless sintering using Y_2O_3 as a sintering additive. Materials sintered at 1870 °C consisted of relatively fine elongated SiO_2 containing AlN polytypoids grains embedded in equi-axed AlN matrix. The Vickers hardness of the composites increased corresponding to a linear mixing of pure AlN and SiO_2 containing 27R polytypoid. The Young's modulus showed a maximum at 3.7 mol% Al_2O_3 and 30 vol.% AlN polytypoids. Both the bending strength and fracture toughness of the polytypoid composites were higher than for pure AlN. Toughening is mainly caused by crack deflection due to residual strain in the microstructure. Further toughening of AlN by elongated polytypoids will be dependent on optimization of the grain size and grain boundary phases.

Acknowledgements

Financial support from The Research Council of Norway is acknowledged. Supported by the Research Council of Norway.

References

[1] J.W. McCauley, N.D. Corbin, High temperature reactions and microstructures in the Al_2O_3–AlN system, in: F.L. Riley (Ed.), Progress in Nitrogen Ceramics, Martinus Nijhoff Publishers, Boston, 1983, pp. 111–118.

[2] L. Dumitrescu, B. Sundman, A thermodynamic reassessment of the Si–Al–O–N system, J. Eur. Ceram. Soc. 15 (1995) 239–247.

[3] C. Qui, R. Metselaar, Phase relations in the aluminum carbide–aluminum nitride–aluminum oxide system, J. Am. Ceram. Soc. 80 (8) (1997) 2013–2020.

[4] P. Tabary, C. Servant, Thermodynamic reassessment of the AlN–Al2O3 system, Calphad 22 (2) (1998) 179–201.

[5] I.-L. Tangen, Y.D. Yu, T. Grande, R.Høier, M.-A. Einarsrud, Phase relations and microstructural development of aluminum nitride–aluminum nitride polytypoid composites in the AlN–Al_2O_3–Y_2O_3 system, J. Am. Ceram. Soc. (in press).

[6] A.D. Westwood, R.A. Youngman, M.R. McCartney, A.N. Cormack, M.S. Notis, Oxygen incorporation in aluminum nitride via extended defects. Part III. Reevaluation of the polytypoid structure in the aluminum nitride–aluminum oxide binary system, J. Mater. Res. 10 (10) (1995) 2573–2585.

[7] Y. Yan, M. Terauchi, M. Tanaka, Structures of polytypoids in AlN crystals containing oxygen, Phil. Mag. A77 (4) (1998) 1027–1040.

[8] K. Komeya, H. Inoue, A. Tsuge, Role of Y_2O_3 and SiO_2 additions in sintering of AlN, J. Am. Ceram. Soc. 57 (9) (1974) 411–412.

[9] P. Tabary, C. Servant, J.A. Alary, Microstructure and phase transformation in the AlN–Al_2O_3 pseudo-binary system, J. Eur. Ceram. Soc. 20 (2000) 913–926.

[10] P.F. Becher, S.-L. Hwang, C.-H. Hsueh, Using microstructure to attack the brittle nature of silicon nitride ceramics, MRS Bull. 2 (1995) 23–27.

[11] S.-G. Lee, Y.-W. Kim, M. Mitomo, Relationship between microstructure and fracture toughness of toughened silicon carbide ceramics, J. Am. Ceram. Soc. 84 (6) (2001) 1347–1353.

[12] S.R. Witek, G.A. Miller, M.P. Harmer, Effects of CaO on the strength and toughness of AlN, J. Am. Ceram. Soc. 72 (3) (1987) 469–473.

[13] J.-L. Huang, J.-M. Jih, Investigation of SiC–AlN. Part II. Mechanical properties, J. Am. Ceram. Soc. 79 (5) (1996) 1262–1264.

[14] E. Hagen, Y.D. Yu, T. Grande, R. Høier, M.A. Einarsrud, Sintering of AlN ceramics using CaO–Al_2O_3 as sintering additive—chemistry and microstructural development, J. Am. Ceram. Soc. 85 (1) (2002) 2971–2976.

[15] S.A. Mariano, D. Friel, I. Bar-On, Elevated temperature mechanical properties of SiC–AlN particulate composites, Ceram. Eng. Proc. 14 (1993) 1077–1088.

[16] J. Tatami, K. Komeya, T. Meguro, S. Iwasawa, R. Terao, Fracture behaviour of strengthened AlN, Ceram. Trans. 106 (2000) 494–499.

[17] M. Tajika, H. Matsubara, W. Rafaniello, Microstructures and properties in aluminium nitride–titanium nitride composite ceramics, Mater. Lett. 41 (1999) 139–144.

[18] J.-L. Huang, J.-M. Jih, Investigation of SiC–AlN. Part I. Microstructure and solid solution, J. Mater. Res. 10 (1995) 651–658.

[19] M.A. Kuzenkova, P.S. Kislyi, O.V. Pshenichaya, Structure and properties of composites based on Ti, Zr and Al nitrides, Inorg. Mater. 12 (1976) 371–374.

[20] Y.G. Tkachenko, D.Z. Yirchenko, G.S. Oleinik, O.A. Shevchenko, S.A. Satanin, Self-reinforced materials based on aluminium nitride, Sov. Powder Metall. 31 (1992) 785–789.

[21] T. Sakai, High-temperature strengths of AlN hot-pressed with Al_2O_3 additions, J. Am. Ceram. Soc. 64 (3) (1981) 135–137.

[22] K.H. Jack, SiAlON ceramics: retrospect and prospect, Mater. Res. Soc. Symp. Proc. 287 (1993) 15–27.

[23] T. Yagi, K. Shinozaki, N. Mizutani, M. Kato, Thermal diffusivity of SiO_2 and Y_2O_3 added AlN ceramics, J. Mater. Sci. 24 (1989) 1332–1336.

[24] T. Yagi, K. Shinozaki, N. Ishizawa, N. Mizutani, M. Kato, Effect of silicon dioxide on the thermal diffusivity of aluminum nitride, J. Am. Ceram. Soc. 71 (7) (1988) 334–338.

[25] P.S. de Baranda, A.K. Knudsen, E. Ruh, Effect of silica on the thermal conductivity of aluminum nitride, J. Am. Ceram. Soc. 76 (7) (1993) 1761–1771.

[26] G. van Tendeloo, K.T. Faber, G. Thomas, Characterization of AlN ceramics containing long-period polytypes, J. Mater. Sci. 18 (1983) 525–532.

[27] P.L. Wang, W.Y. Sun, D.S. Yan, Mechanical properties of AlN-polytypoids—15R, 12H and 21R, Mater. Sci. Eng. A272 (1999) 351–356.

[28] S. Hæreid, E. Nilsen, M.-A. Einarsrud, Properties of silica gels aged in TEOS, J. Non-Cryst. Solids 204 (1996) 228–234.

[29] O. Herstad, K. Motzfeldt, Vapour pressures in the system Al–Al_2O_3. The effusion method and pressure compensation methods, Rev. Hautes Temper. Et Réfract 3 (1966) 291–300.

[30] M. Mitomo, M. Tsutsumi, H. Tanaka, S. Uenosono, F. Saito, Grain growth during gas-pressure sintering of β-silicon nitride, J. Am. Ceram. Soc. 73 (8) (1990) 2441–2445.

[31] F. Sass, C. Bouché, A. Leitner, Dubbels Taschenbuch für den Maschinenbau, Springer-Verlag, Berlin, 1961.

[32] ISO/CD 15732 fine ceramics (advanced ceramics, advanced technical ceramics)—test method for fracture toughness at room temperature by single edge precracked beam (SEPB) method, International Organization for Standardization, Geneva, Switzerland.

[33] I.-L. Tangen, Y.D. Yu, T. Grande, T. Mokkelbost, R. Høier, M.-A. Einarsrud, Preparation and characterisation of aluminium nitride–silicon carbide composites, Ceram. Int. 30 (2004) 931–938.

[34] I.-L. Tangen, Y.D. Yu, T. Grande, R. Høier, M.-A. Einarsrud, Preparation and characterisation of aluminium nitride–titanium nitride composites, J. Eur. Ceram. Soc. 24 (2004) 2169–2179.

[35] G.R. Anstis, P. Chantikul, B.R. Lawn, D.B. Marshall, A critical evaluation of indentation techniques for measuring fracture toughness. I. Direct crack measurements, J. Am. Ceram. Soc. 64 (9) (1981) 533–538.

[36] J. Gröbner, H.L. Lukas, F. Aldinger, Thermodynamic calculations of the quasibinary Al_2O_3–Y_2O_3 system and the Y–Al–O ternary system, Z. Metallkd. 87 (1996) 268–273.

[37] W.Y. Sun, Z.K. Huang, T.Y. Tien, T.S. Yen, Phase relationships in the system Y–Al–O–N, Mater. Lett. 11 (3/4) (1991) 67–69.

[38] D.D. Marchant, T.E. Nemecek, Aluminium nitride: preparations, processing and properties, in: M.F. Yan, K. Niwa, H.M. O'Bryan, W.S. Young (Eds.), Advances in Ceramics: Ceramic Substrates and Packages for Electronic Applications, Am. Ceram. Soc. Inc., Westerville, OH, 1989, pp. 19–54.

[39] H. Hunold, Herstellung, Eigenschaften und Anwendungsmöglichkeiten von Aluminiumnitrid-Bauteilen, Metallurgy 3 (1990) 266–269.

[40] N.H. Kim, Q.D. Fun, K. Komeya, T. Meguro, Phase reaction and sintering behaviour in the pseudoternary system AlN–Y_2O_3–Al_2O_3, J. Am. Ceram. Soc. 79 (10) (1996) 2645–2651.

[41] N.H. Kim, K. Komeya, T. Meguro, Effect of Al_2O_3 addition on phase reaction of the AlN–Y_2O_3 system, J. Mater. Sci. 31 (1996) 1603–1608.

[42] T. Shirakami, K. Urabe, H. Nakano, T. Meguro, K. Komeya, N.H. Kim, Microstructural evolution during sintering of aluminum nitride ceramics doped with alumina and yttria, J. Am. Ceram. Soc. 84 (3) (2001) 631–635.

[43] W.D. Kingery, H.K. Bowen, D.R. Uhlmann, Introduction to Ceramics, John Wiley & Sons, New York, 1976.

[44] K.T. Faber, A.G. Evans, Crack deflection processes. I. Theory, Acta Met. 31 (1983) 565–576.

[45] K.T. Faber, A.G. Evans, Crack deflection processes. II. Experiment, Acta Met. 31 (1983) 577–584.